Appl Phys B (2010) 98: 93–98
DOI 10.1007/s00340-009-3705-7

Applied Physics B
Lasers and Optics

Three-dimensional photonic microstructures produced by electric field assisted dissolution of metal nanoclusters in multilayer stacks

V. Janicki · J. Sancho-Parramon · F. Peiró · J. Arbiol

Received: 2 April 2009 / Revised version: 9 July 2009 / Published online: 12 September 2009
© Springer-Verlag 2009

Abstract The formation of three dimensional (3D) photonic microstructures by the locally selective dissolution of metal clusters embedded in dielectric multilayer stacks is presented. Dissolution of clusters is performed by the simultaneous application of electric field and temperature. The produced photonic structures show a highly tailorable optical behavior that combines the interferential effects of multilayer stacks and the surface plasmon resonance of non-dissolved metal clusters. Due to its feasibility and the possibility to widely modify the optical properties of the resulting structures, the current approach represents a promising method for the production of novel components based on 3D-metallodielectric photonic structures.

PACS 68.65.Ac · 36.40.Vz · 42.25.Hz · 42.79.-e · 81.07.-b

1 Introduction

Composite materials consisting of metal particles embedded in a dielectric matrix show striking linear and nonlinear optical properties due to the surface plasmon resonance (SPR) of metal free electrons. Since the SPR characteristics strongly depend on the particle size, shape and spatial distribution [1], the possibility of structuring metallodielectric composites is very attractive. In particular, three-dimensional (3D) metallodielectric photonic structures show outstanding electromagnetic properties such as large photonic bandgap [2], tailored thermal emission [3] and negative refractive index [4]. Thus, 3D structure-based photonic devices are applied in fields like enhanced resonance sensing [5], photovoltaics [6] and waveguiding [7]. The most widely used techniques for production of 3D metallodielectric structures are laser-based methods [8], self-assembly approaches [9] or e-beam lithography [10]. Although these methods offer precise structuring capabilities, it is difficult to implement them in large-scale production processes as they are often expensive and time consuming. Therefore, a basic challenge for the practical development of components based on 3D photonic structures is the quest for cheaper and easy-to-extend structuring techniques.

In the present study, we explore the possibility to fabricate metallodielectric 3D structures based on the electric field assisted dissolution (EFAD) of metal clusters. It has been shown that the simultaneous application of static electric field and moderately elevated temperature induces dissolution of metallic nanoparticles embedded in a glass matrix [11] or film [12, 13]. The same phenomenon has been observed for metal islands deposited on a glass substrate [14]. The dissolution process can be controlled locally by applying the electric field with patterned electrodes, resulting in the production of two-dimensional photonic structures in glasses containing nanoparticles [15, 16]. We have applied the EFAD technique to different types of multilayer thin film stacks with embedded metal nanoparticles. The multilayer stacks, representing a one-dimensional structure,

V. Janicki (✉) · J. Sancho-Parramon
Institute Ruđer Bošković, Bijenička cesta 54, 10000, Zagreb, Croatia
e-mail: janicki@irb.hr
Fax: +385-1-4680104

F. Peiró
TEM-MAT, Serveis Cientificotècnics, Universitat de Barcelona, Lluís Solé i Sabarís 1-3, 08028, Barcelona, CAT, Spain

J. Arbiol
ICREA Research Professor at Institut de Ciència de Materials de Barcelona, CSIC, 08193, Bellaterra, CAT, Spain
e-mail: arbiol@icrea.cat

consist of a combination of dielectric thin films with nanometric metal clusters deposited at interfaces between films or embedded within films. It shall be shown that in such samples, a 3D structure can be generated by selective dissolution of embedded metal clusters using two-dimensional EFAD patterning. In addition to the SPR-related properties, the optical behavior of the resulting 3D structure can also be tailored by the interference phenomena that take place within the multilayer stack. From a technological point of view these 3D structures can be fabricated easily, as their production requires the combination of well established thin film deposition processes and the EFAD technique.

2 Experimental

Multilayer stacks used for fabricating 3D structures were prepared by electron beam evaporation on glass (BK7) substrates. The stacks were made of dielectric SiO_2 or TiO_2 thin films. Few nanometers of Ag were deposited between each dielectric film. Due to the small amount of deposited material, the metal does not form a compact film but is structured as nanometric islands [14, 17, 18]. In order to induce EFAD structuring, the samples were annealed for two hours at 250°C with simultaneous application of a constant voltage of 1 kV. The multilayer stack was facing the anode. Cr thin films deposited on glass substrates were used as electrodes to assure smooth contact with the sample surface. The anode was patterned by microphotolithography into a diffraction grating with 28 lines/mm and line thickness 16 microns. In this way, the sample areas in contact with the grating lines were exposed to both electric field and temperature (zones A) and the regions out of contact were exposed to temperature only (zones B). Optical characterization of the samples was performed by UV–VIS–NIR spectrophotometry and morphological and chemical characterization was done by scanning transmission electron microscopy (STEM) in high angle annular dark field (HAADF) mode, in a Jeol2010F field-emission Gun Microscope. In order to perform the chemical characterization of our 3D structures, we used electron energy-loss spectroscopy (EELS) with a GATAN GIF2000 coupled to the previous microscope. Diffraction patterns of the generated structures were measured in the UV–VIS–NIR spectral range with a VASE ellipsometer (J.A. Woollam) working in scatterometry mode.

3 Results and discussion

As deposited, samples were opaque owing to the strong SPR absorption of the electrons of metal islands. In a similar way to the previous EFAD experiments [11–14], due to the treatment, clusters dissolve, SPR disappears and, as a result, zones A of the samples become bleached. Figure 1 shows transmission optical microscopy pictures of the grating used as electrode (Fig. 1(a)) and treated sample with a multilayer consisting of 5 pairs of Ag and SiO_2 films (BK7/$(Ag/SiO_2)^5$) with thickness of 7 nm of Ag and 100 nm of SiO_2 (Fig. 1(b)). It can be seen that the pattern of the electrode has been imprinted in the multilayer sample. Figure 1(c) shows the sample obtained by repeated EFAD treatment with the grating electrode rotated 90° with respect to the first treatment, resulting in a regular pattern of opaque squares. Thus, a 3D structure is generated by applying the two-dimensional EFAD-induced patterning to the one dimensional structure defined by the multilayer stack. The structuring was applied to different types of multilayer stacks with embedded silver clusters. The thickness of the dielectric films was in the range between few nanometers and a half of a micron. This is the typical range for film thickness used in interferential filters in the visible and infrared range, where the SPR of noble metals takes place. For all samples, full bleaching of the zones A was achieved at the above mentioned conditions (application of 1 kV at 250°C for two hours). It must be mentioned that structuring was obtained only above some threshold values of applied electric field and temperature, which is in agreement with previous EFAD experiments in glass containing metal nanoparticles [19]. Similarly, partial bleaching was achieved when the treatment time was too short, depending on the sample characteristics [19, 20]. The precise influence of EFAD parameters, materials and substrate type to the structuring process is currently investigated and will be discussed elsewhere. It was observed that the sample surface showed nano-imprints (up to few tens of nanometers in depth) in the regions where

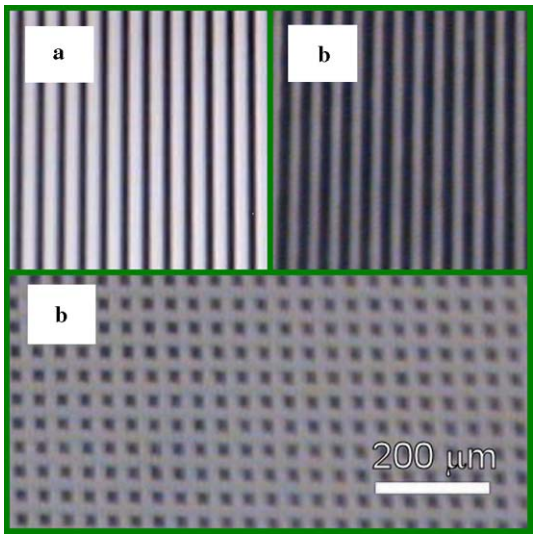

Fig. 1 Optical microscopy pictures of the grating used as electrode (**a**), multilayer sample after EFAD process (**b**) and multilayer sample after two consecutive EFAD treatments, with the electrode rotated 90° in the second treatment (**c**)

the electric field was applied (zones A). Such imprints have been observed recently in two-dimensional structures generated by EFAD in nanocomposites glass [16, 21]. The nature of the nano-imprints has been associated (i) to stress relaxation due to the presence of silver ions instead of silver atoms upon particle dissolution and (ii) to the migration of alkali ions in glass under the influence of electric field and the formation of an ion-depleted region. For the samples investigated in this study, there are no alkali ions in the multilayer structure but in the BK7 (soda-lime) substrate. The origin of the surface nano-imprinting and its dependence with the treatment parameters will be a topic of future research.

Transmittance spectra were taken to check in more detail how the optical behavior of the sample changes after EFAD treatment (Fig. 2). The high transmittance in zone A evidences the complete absence of SPR. In addition, fringes appearing in the transmittance spectra of this zone suggest interference effects associated with the multilayer stack. In zone B, transmittance of the sample is low owing to SPR absorption of non-dissolved metal islands. The absorption in this case is blue-shifted and less intense than for the as-deposited sample. Such behavior can be explained by a reduction of the metal fraction in the multilayer stack [8]. Cross-section high angular annular dark field (HAADF or Z-Contrast) scanning transmission electron microscopy (STEM) micrographs of zones A and B of the multilayer structure were taken in order to verify the dissolution process. In zone A (Fig. 3(a)), no Ag islands can be detected at any of the interfaces between SiO_2 films, meaning the particles have been completely dissolved. Additionally, the interface appears to have a lower electronic density than the SiO_2 films. In zone B (Fig. 3(b)), the multilayer stack consists of SiO_2 films with Ag nanometric clusters located at the interface between the films. Therefore, the three dimensional nature of the obtained structure is confirmed, with zones B and A being multilayer stacks with and without silver islands at the interfaces between layers, respectively.

The cluster dissolution phenomenon has been discussed previously [11–15, 19] and can be summarized as follows: Metal clusters are ionized under the influence of high electric field, with electrons tunneling to the anode. Due to the electric field, the positively charged silver ions can then be ejected from the silver cluster into the dielectric environment, leaving uncharged clusters. This process continues until the cluster is completely dissolved. In order to get a deeper insight to the modifications induced by this process, composition of the films was analyzed by electron energy loss spectroscopy (EELS) profiles taken in direction perpendicular to the interface between SiO_2 films (Fig. 4). The relative composition in zone A (Fig. 4(a)) is approximately constant throughout the SiO_2 films and the region in which Ag islands were dissolved. Thus, the lower electronic density of the interface revealed by STEM is not due to a different

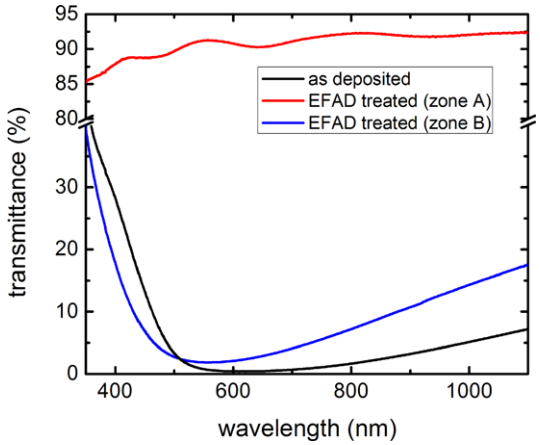

Fig. 2 Transmittance spectra of the multilayer structure BK7/$(Ag/SiO_2)^5$: as deposited sample (*black line*), zone A (*red line*) and B (*blue line*) of the treated sample

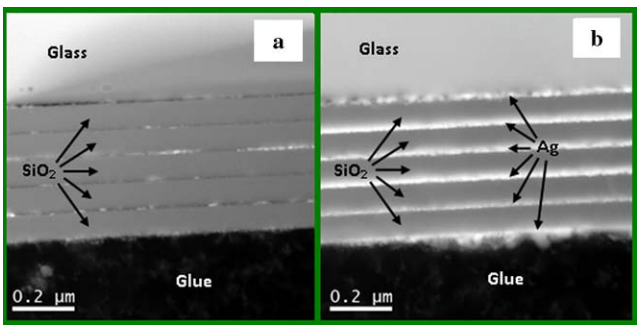

Fig. 3 Cross-section HAADF STEM micrographs of the EFAD-treated multilayer structure: (**a**) zone A and (**b**) zone B

composition, but to the presence of material with lower density than the SiO_2 films, i.e., porous SiO_2. The low-density SiO_2 nature of the interface is supported by the interference fringes observed in the transmittance spectra of zones A that appear due to a lower refractive index of the interface. Formation of pores upon EFAD treatment has been observed previously in nanocomposite glass [21, 22]. Ag is dispersed through the SiO_2 films (bright spots in Fig. 4(a) inset), corresponding to the Ag ions that have been ejected from the islands towards the dielectric environment. Particles or clusters are not present in these Ag-rich regions, confirming that the dissolution process is an atom-by-atom process as previously suggested [11, 14]. Nevertheless, due to their lower conductivity in purely dielectric film than in soda-lime glass [14], the ions are not drifted away and collect to form a percolated silver layer in opposition to the behavior observed in metal-doped glasses [23]. Composition of the interfaces in zones B (Fig. 4(b)) consists of Ag associated to the islands and Si and O corresponding to SiO_2 filling the space between islands. However, the detected amount of O at the interface is much higher than for stoichiometric SiO_2. This suggests that Ag islands could be partially oxidized upon

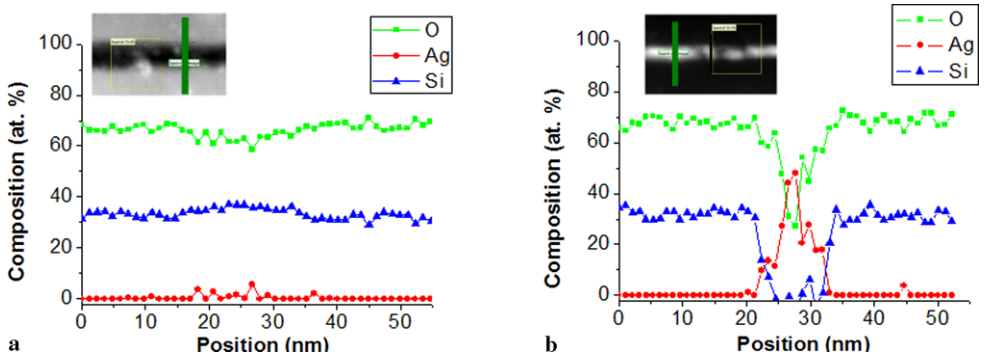

Fig. 4 EELS profiles of the zone A (**a**) and B (**b**) of the multilayer structure taken around the interface between SiO_2 films. Insets show STEM micrographs in which EELS spectra were taken (*green lines*)

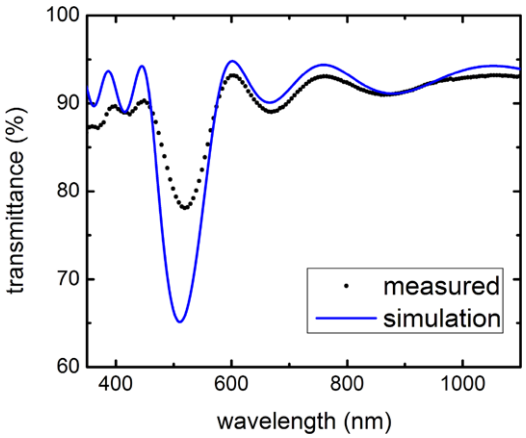

Fig. 5 Optical transmittance spectra of zone A of the multilayer structure consisting of substrate/$(X/SiO_2)^5$, in which X represents a multilayer of Ag and SiO_2 films (see text for details) after EFAD treatment (*black dots*) and simulation of an equivalent structure assuming that after EFAD treatment Ag islands are replaced by pores (*blue line*)

thermal treatment, as previously observed [24]. Silver oxidization represents a decrease of the filling factor of the material with metallic behavior and thus explains the intensity reduction and blue-shift of the SPR absorption observed in zones B with respect to the original sample (Fig. 2).

In addition to the just described 3D structures in which the metal clusters are located at the interface between films, by application of one or two dimensional EFAD patterning it may be possible to generate structures in which the clusters are located in wires or cuboids. For this purpose, a multilayer sample with metal clusters distributed within the whole thickness of some films was prepared and studied. The multilayer structure was substrate/$(X/SiO_2)^5$ in which X represents a 100 nm thick SiO_2:Ag composite film formed by the sequential deposition of 5 nm of Ag and 20 nm of SiO_2. The pure SiO_2 layers of the multilayer stack were 80 nm thick. The transmittance of zone A of this sample after the EFAD treatment is presented in Fig. 5. Due to the larger thickness of the layers where particles are dissolved, interferential fringes are enhanced with respect to those of the sample shown in Fig. 2. Taking into account the deposited thicknesses, the theoretical transmittance spectrum of an equivalent multilayer stack is shown for comparison. The refractive index of SiO_2 was taken from literature (∼1.45 in the measured spectral range) [25] and for the X layers was computed assuming a mixture of SiO_2 and air and applying effective medium theory [26], with relative volume ratios equal to the deposited SiO_2:Ag thickness ratio (refractive index around ∼1.35 in the considered spectral range). The extinction coefficient of SiO_2 and SiO_2-air mixture is negligible in the measured spectral range. Previously, it has been reported that the presence of diffused Ag ions may substantially increase the refractive index of silica (up to 0.1 refractive index units) [27]. However, due the relatively low concentration of Ag ions in the studied samples, the refractive index increase is expected to be much smaller. In a qualitative comparison between data and simulation, such an increase can be neglected. The most pronounced interference fringe appears around 500 nm, that corresponds approximately to the average wavelength in which the SiO_2 layers and X layers are quarterwaves, leading to destructive interference conditions and reflecting the incident light. Since the contrast between the refractive index of the X and SiO_2 layers is low, the amount of transmitted light drops to only 65% for the simulated structure. There is a remarkable agreement between simulation and experimental data in the wavelength position of the interference fringes. However, the amplitude of the fringes is smaller in the experimental data than in the simulated data. The simulation assumes a plane-parallel interface between X and SiO_2 films. However, as observed by STEM, the interfaces are rough and can scatter light, reducing the amount of transmitted light and weakening the interferential effects. Light scattering increases as the ratio between the size of roughness features, and the wavelength is higher [28], therefore becoming more important for short wavelengths, as observed experimentally. In any case, the optical measurements show total absence of SPR and indicate the complete dissolution of clusters, as well as the presence of remarkable interferential effects. The application of two-dimensional EFAD patterning to this sample suggests the possibility to generate plasmonic cuboids formed by metal particles embedded in dielectric film. The length, width and lateral separation of these cuboids could be controlled by the

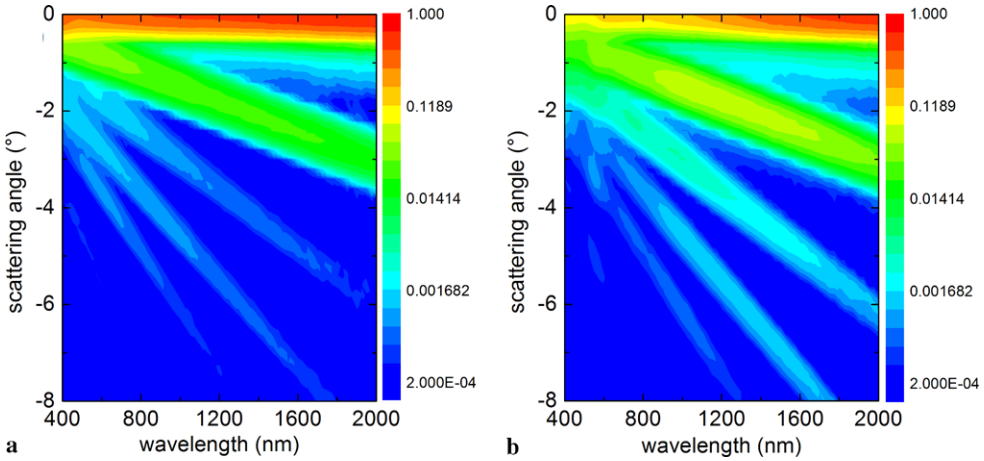

Fig. 6 Wavelength-dependence of diffraction pattern of multilayer structures produced by EFAD treatment: (**a**) multilayer structure BK7/$(Ag/SiO_2)^5$ with thickness of 7 nm of Ag and 100 nm of SiO_2 and (**b**) multilayer structure BK7/$(X/SiO_2)^5$, in which X represents a multilayer of Ag and SiO_2 films

electrode pattern while the height, vertical separation and composition of cuboids would be determined by the film deposition process.

In order to illustrate some of the photonic properties of the generated microstructures, Fig. 6(a) shows the wavelength-dependence of the transmitted diffraction pattern of the grating of sample from Fig. 1(b). The first few diffraction orders as well as the non-diffracted (zeroth order) beam are observed. It can be seen that near the surface plasmon resonance peak (around 500–600 nm as shown in Fig. 2), the non-diffracted beam has a minimum, while the other diffraction orders have a maximum. In this spectral region, the grating lines are highly absorbing due to the metal nanoparticles surface plasmon resonance and there is a strong contrast between the transmittance of the opaque and transparent regions of the generated structure. Away from the surface plasmon resonance peak, the grating lines are less absorbing and the contrast between transparent and opaque regions is smaller, leading to a lower grating efficiency. Thus, the ratio between the intensity of the first and zeroth orders is 12.5% at 500 nm, while at 400, 1000 and 2000 nm it is 8.5%, 6.0% and 2.5%, respectively. Since the diffraction properties of the multilayer grating depend on the SPR-related absorption, these properties can be widely tailored, modifying the SPR lineshape by the deposition conditions of metal clusters [14], the number of deposited island films and the thickness of the separating dielectric films [17].

Figure 6(b) shows the diffraction patterns for a grating produced by EFAD of the sample with multilayer structure substrate/$(X/SiO_2)^5$ described before. In this case, the diffraction orders are wavelength-modulated and present different intensity maxima and minima. The ratio between the first and zeroth order diffracted beams intensity at 400, 500, 1000, and 2000 nm are 26, 28, 36, and 6%, i.e., the maximum efficiency is not achieved around the plasmon resonance peak as for the example of Fig. 6(a). Such difference is attributed to the interplay between the wavelength-dependence of the transmission behavior of the opaque and transparent regions which are strongly affected by interference effects (Fig. 5). This observation confirms that the optical behavior of the EFAD-produced structures can be further tailored by interferential properties of multilayers stacks, in addition to the surface plasmon resonance properties of non-dissolved nanoparticles. A quantitative description of the optical behavior of these structures would require the use of appropriate numerical methods as has been recently done for two-dimensional photonic slabs having finite thickness, where interferential or waveguiding effects have been observed [29, 30].

4 Conclusions

We have demonstrated the fabrication of 3D microstructures by electric field assisted dissolution of metal clusters embedded in multilayer stacks. The application of moderately elevated temperatures and intense electric field leads to the dissolution of islands deposited at the interface between dielectric films. Silver diffuses into the dielectric surrounding, creating pores in the regions where islands were previously located. In the regions where islands are dissolved, no SPR is observed and the optical properties of the sample are changed drastically. The dissolution process can be controlled selectively by applying the electric field with patterned electrodes. Thus, 3D structuring can be obtained by combining the one dimensional multilayer structure with the two-dimensional EFAD-induced pattern. Metal clusters are present in the 3D structures as bidimensional ensembles, when deposited at the interface between films, or cuboids, when clusters are distributed through the thickness of films. In addition to the SPR-based metallodielectric properties, the optical behavior of the sample can be further tailored by the interferential effects. Multilayer thin film stacks enable the design of a wide variety of components with different optical performances: band-pass filters, mirrors, polarizers,

etc. The generation of 3D structures from these well-known components could facilitate the design of a new generation of photonic structures. In addition, the SPR-properties of metal island films can be tuned by controlling the deposition conditions (thickness, substrate temperature, dielectric environment). The production of these structures could be done at low costs and easily implemented in mass-production processes, as it requires well-established thin film deposition technology and inexpensive EFAD technique.

References

1. U. Kreibig, M. Vollmer, *Optical Properties of Metal Clusters*. Springer Series in Material Science. Springer, Berlin (1995)
2. A. Moroz, Phys. Rev. Lett. **83**, 5274 (1999)
3. J.-H. Lee, Y.-S. Kim, K. Constant, K.-M. Ho, Adv. Mater. **19**, 791 (2007)
4. R.A. Shelby, D.R. Smith, S. Schulz, Science **292**, 77 (2001)
5. H.M. Chen, L. Pang, A. Kher, Y. Fainman, Appl. Phys. Lett. **94**, 073117 (2009)
6. S.Y. Lin, S. Moreno, G.R. Fleming, Appl. Phys. Lett. **83**, 380 (2003)
7. J.R. Krenn, Nat. Mater. **2**, 210 (2003)
8. A. Podlipensky, A. Abdolvand, G. Seifert, H. Graener, Appl. Phys. A **80**, 164 (2005)
9. Y. Wang, M. Ibisate, A.-Y. Li, Y. Xia, Adv. Mater. **18**, 471 (2006)
10. A. Hohenau, H. Ditlbacher, B. Lamprecht, J.R. Krenn, A. Leitner, F.R. Aussenegg, Microelectron. Eng. **83**, 1464 (2006)
11. A. Podlipensky, A. Abdolvand, G. Seifer, H. Graener, O. Deparios, P.G. Kazansky, J. Phys. Chem. B **108**, 17699 (2004)
12. F.P. Mezzapesa, I.C.S. Carvalho, P.G. Kazansky, O. Deparis, M. Kawazu, K. Sakaguchi, Appl. Phys. Lett. **89**(18), 183121 (2006)
13. Z. Zou, X. Chen, Q. Wang, S. Qu, X. Wang, J. Appl. Phys. **104**, 113113 (2008)
14. J. Sancho-Parramon, V. Janicki, J. Arbiol, H. Zorc, F. Peiró, Appl. Phys. Lett. **92**, 163108 (2008)
15. A. Abdolvand, A. Podlipensky, S. Matthias, F. Syrowatka, U. Gösele, G. Seifert, H. Graener, Adv. Mater. **17**, 2983 (2005)
16. A.A. Lipovskii, M. Kuittinen, P. Karvinen, K. Leinonen, V.G. Melehin, V.V. Zhurikhina, Y.P. Svirko, Nanotechnology **19**, 415304 (2008)
17. S. Kachan, O. Stenzel, A. Ponyavina, App. Phys. B: Lasers Opt. **84**, 281 (2006)
18. P. Heger, O. Stenzel, N. Kaiser, Proc. SPIE **21**, 5250 (2004)
19. O. Deparis, P.G. Kazansky, A. Podlipensky, A. Abdolvand, G. Seifert, H. Graener, J. Appl. Phys. **100**, 044318 (2006)
20. H. Graener, A. Abdolvand, S. Wackerow, O. Kiriyenko, W. Hergert, Phys. Stat. Sol. (a) **204**, 3838 (2007)
21. M. Leitner, H. Peterlik, B. Sepiol, H. Graener, M. Beleites, G. Seifert, Phys. Rev. B **79**, 153408 (2009)
22. J. Sancho-Parramon, A. Abdolvand, A. Podlipensky, G. Seifert, H. Graener, F. Syrowatka, Appl. Opt. **45**, 8874 (2006)
23. A. Abdolvand, A. Podlipensky, G. Seifert, H. Graener, O. Deparis, P. Kazansky, Opt. Express **13**, 1266 (2005)
24. M.X. Yang, P.W. Jacobs, C. Yoon, L. Muray, E. Anderson, D. Attwood, G.A. Somorjai, Catal. Lett. **45**, 5 (1997)
25. E.D. Palik, *Handbook of Optical Constants* (Academic Press, San Diego, 1991)
26. J. Sancho-Parramon, V. Janicki, J. Phys. D, Appl. Phys. **41**, 215304 (2008)
27. R.V. Ramaswamy, R. Srivastava, J. Lightwave Tech. **6**, 984 (1988)
28. C.K. Carniglia, D.G. Jensen, Appl. Opt. **41**, 3167 (2002)
29. Z. Kral, L. Vojkuvka, E. García-Caurel, J. Ferré-Borrull, L.F. Marsal, J. Pallarés, Photonics Nanostruct. **7**, 12 (2009)
30. Z. Kral, J. Ferré-Borrull, T. Trifonov, L.F. Marsal, A. Rodriguez, J. Pallares, R. Alcubilla, Thin Solid Films **516**, 8059 (2008)